Published in final edited form as:

J Neurosci Methods. 2013 June 15; 216(2): 142–145. doi:10.1016/j.jneumeth.2013.04.001.

Photoacoustic and optical coherence tomography of epilepsy with high temporal and spatial resolution and dual optical contrasts Type of article: research article

Vassiliy Tsytsarev, Ph.D.[1,2,4], **Bin Rao, Ph.D.**[1,4], **Konstantin I. Maslov, Ph.D.**[1,4], **Li Li, Ph.D.**[1,3], and **Lihong V. Wang, Ph.D.**[1,*]

[1]Optical Imaging Laboratory, Department of Biomedical Engineering, Washington University in St. Louis, One Brookings Drive, St. Louis, MO 63130

[2]University of Maryland School of Medicine, Department of Anatomy and Neurobiology 20 Penn St, HSF-II, Baltimore, MD 22201

[3]Massachusetts General Hospital, Harvard Medical School, Wellman Center for Photomedicine 40 Parkman Street, Room 160, Ruth Sleeper Hall, Boston, MA 02114

Introduction

Epilepsy results from “electrical storms” inside the brain that cause recurring seizures. About 2 in 100 people in the United States experience an unprovoked seizure at least once in their lives. The population and shape of involved epileptic neurons vary along the time course of each epileptiform event in a very short time span. Current clinical functional imaging methods, such as functional magnetic resonance imaging (fMRI), positron emission tomography (PET) and single-photon emission computed tomography (SPECT), are limited by their low temporal resolution in documenting such paroxysmal epileptiform events. High temporal resolution is critical to overcome the motion artifacts caused by patients or procedures during epilepsy surgery. Although optical mapping methods such as intrinsic optical imaging (IOS) (Bahar *et al*,. 2006; Inyushin *et. al.*, 2001; Haglund and Hochman, 2004; Schwartz *et al.*, 2004; Schwartz and Bonhoeffer 2001) and voltage-sensitive dye imaging (VSD) (Cohen *et. al*,. 1986) have limitations in imaging depth and tissue toxicity,

Corresponding author: lhwang@wustl.edu.

[4]These authors contribute equally to this manuscript

Vassiliy Tsytsarev, Ph.D., University of Maryland School of Medicine, Department of Anatomy and Neurobiology, HSF II Room S251, 20 Penn Street, Baltimore, MD 21201-1075 Tel: (410) 706-8907, tsytsarev@umaryland.edu

Bin Rao, Ph.D., Department of Biomedical Engineering, Washington University in St. Louis, One Brookings Drive, St. Louis, Missouri 63130, Phone: (314) 935-4911, raob@seas.wustl.edu

Konstantin Maslov, Ph.D., Department of Biomedical Engineering, Washington University in St. Louis, One Brookings Drive, St. Louis, Missouri 63130, Phone: (314) 935-4911, kimaslov@biomed.wustl.edu

Li Li, Ph.D., Massachusetts General Hospital, Harvard Medical School, Wellman Center for Photomedicine, 40 Parkman Street, Room 160, Ruth Sleeper Hall, Boston, MA 02114, Department of Biomedical 63130, Phone: (617) 643-5310, li.li@mgh.harvard.edu

Lihong V. Wang (Corresponding Author), Department of Biomedical Engineering, Washington University in St. Louis, One Brookings Drive, St. Louis, Missouri 63130, Phone: (314) 935-4911, lhwang@seas.wustl.edu

the development of epileptic animal models has made them very useful (Raol *et. al.*, 2012). More recent developments in the optical mapping of neural activities include the optical coherence tomography (OCT) (Satomura Y. *et. al.*, 2004; Aguirre A. D. *et. al.*, 2006; Rajagopalan U. M. *et. al.*, 2007; Chen Y. *et. al.*, 2009; Sato M. *et. al.*, 2010; Liang *et. al.*, 2011; Lenkov *et. al.*, 2012; M. Eberle *et. al.*, 2012) and photoacoustic microscopy (PAM) (Hu *et. al.*, 2009; Maslov *et. al.*, 2008; Tsytsarev *et. al.*, 2011; Wang *et. al.*, 2003; Wang 2008; Wang 2009; Liao *et. al.*, 2010; Liao *et. al.*, 2012a; Liao *et. al.*, 2012b). OCT can image both the refractive index modulation of the tissue that surrounds epileptic neurons with optical scattering contrast and the neuron-vasculature coupled blood flow patterns with Doppler OCT contrast. PAM represents an innovation in the functional imaging of red blood cells and blood flow. It provides functional data such as the oxygen saturation of red blood cells in the microvasculature. Because PAM is based on pure optical absorption contrast, it does not require the dense optical scans required by Doppler OCT, and it is immune to axial motion artifacts that may significantly compromise the blood flow images generated by the Doppler OCT in *in vivo* applications. As a rapidly evolving imaging technology, PAM promises deep imaging into tissue due to its multi-scale imaging capability (Wang *et. al.*, 2012). By recording the optical refractive index modulation with OCT technology and simultaneously documenting the hemodynamic changes in epileptiform events with PAM, we can, for the first time, perform epilepsy mapping with high temporal and spatial resolution and dual optical contrasts. We expect our demonstrated technology to have great utility in applications such as epilepsy drug development and epilepsy surgery.

Materials and Methods

Animal preparations

For each experiment, a Swiss Webster mouse (Hsd: ND4, 25–30 g; Harlan, Indianapolis, IN) was anesthetized by an intraperitoneal (IP) injection of a mixture of ketamine (87 mg/kg) and xylazine (13 mg/kg). The anaesthetized animal was placed in a custom-made stereotaxic head holder, and the left dorsal portion of the skull was exposed by surgically removing the scalp and muscle. A cranial opening (~4–5 mm^2) was made using a dental drill over the left hemisphere, and the exposed dura mater surface was cleaned with artificial cerebrospinal fluid (ACSF). Throughout the experiment, the animal was supplied with breathing-grade compressed air (AI B300, Airgas, MO) and maintained under anesthesia using isoflurane (1.0–1.5% with an airflow rate of ~1 L/min), while the body temperature of the animal was maintained at 37 °C by a temperature-controlled electrical heating pad. After each experiment, the animal was euthanized with an overdose of pentobarbital. All experimental animal procedures were carried out in conformance with the laboratory animal protocol approved by the Animal Studies Committee of Washington University in St. Louis.

Inducement of the epileptic seizures

After craniotomy, 0.35 μL of a 25 mM solution of 4-aminopyridine (4-AP) in artificial cerebrospinal fluid (ACSF) was injected into cortical layers II–III, using an injector device (Nanojet II) with a 15–25 μm diameter glass microcapillary (Bahar et al. 2006; Tsytsarev et al. 2011). The injector was mounted on a micromanipulator that allowed injections 0.2 – 0.3 mm below the dura mater surface. A single channel electroencephalogram (EEG) was

recorded through a screw-type electrode placed in the left hemisphere in the skull, then amplified by an AC/DC differential amplifier (A-M Systems, Model 3000), digitized at 5000 Hz, and recorded. The start of EEG data acquisition was manually initiated.

Optical epilepsy mapping with dual contrasts

A dual modality optical imaging system that can simultaneously provide a co-registered OCT image and a PAM image (Figure 1) was used to provide optical mappings of epilepsy. The OCT imaging channel provided depth-resolved brain tissue structure images based on optical scattering contrast (Rao *et. al.*, 2008). The PAM channel provided depth-resolved brain vasculature images based on optical absorption contrast (Rao *et. al.*, 2010a). OCT and PAM Alines were acquired sequentially for each scanning location. Thus, an OCT image and a PAM image were recorded virtually simultaneously. Each B-scan frame contained 800 scanning points (A-lines). At an imaging speed of 5,000 A-lines-per-second, 500 B-scan frames were acquired within an 80-second time window (Rao *et. al.*, 2010b). Similar to the procedures described in our previous publications (Tsytsarev *et. al.*, 2011; Hu *et. al.*, 2009), we identified two vessels close to the 4-AP injection site and performed repeated B-scans over the selected vessels to map epilepsy in both spatial and time dimensions. The temporal resolution of epilepsy mapping was 6.25 Hz. The spatial lateral resolutions of epilepsy mapping with OCT and PAM were 5.2 μm and 3.5 μm, respectively.

After image acquisition, three types of image data (EEG, OCT, PAM) were analyzed separately. The EEG data was simply displayed as voltage versus time. For the OCT data, the optical scattering signal intensity was calculated by Fourier transformation of the interference fringe recorded by a line-scan CCD camera. Using the first B-scan image as a baseline, we calculated the depth-resolved reflectivity change $\Delta R(x,t)$, where x represents depth and t represents the time or B-scan number, by averaging 800 A-lines within every B-scan image. Then, $\Delta R(x,t)$ was averaged along the imaging depth to generate an averaged reflectivity change over time, $\Delta R(t)$. For PAM data, the A-line amplitude of the photoacoustic signal was extracted via Hilbert transformation. The vessel diameter was directly shown by the maximum amplitude projection (MAP) of PAM B-scan images. Changes in vessel diameter could be directly visualized from the plot of MAP images along the time axis.

Results

After a 4-AP intracortical injection, epileptic seizures occurred periodically for 2 – 4 h, lasting 20 – 200 s at intervals of 2 –20 min. Figure 2A records a typical seizure EEG signal course lasting about 80 seconds. Figures 2B and 2C plot the 1D vertical MAP images from PAM along the horizontal time axis. A large vasodilatation of the blood vessels (veins), as shown in figure 2B, signals the electrographic onset of seizure, which is well-correlated with the EEG signal. The vessel (artery) in figure 2C displays a similar vasodilatation effect, but with reduced amplitude and prolonged duration. It is interesting to note that significant vasodilatation occurred only near the injection site. Outside a cortical area of about 1 mm^2, vasodilatation was below our detection threshold of about 10%. Additionally, it seems that the vasodilatation may signal the beginning of seizure earlier than conventional EEG

signals. From figure 2B, we observed that after the large vessel dilation the vessel was smaller than the baseline diameter. Further study might be interesting, but is beyond the scope of this communication.

The depth-resolved reflectivity change ΔR(x,t) during seizure is shown in figure 2D. From the plot of ΔR(x,t), we can easily visualize the depth-resolved reflectivity change along the whole time course of the seizure. A reflectivity change ΔR(t) averaged along the depth direction at each sampling time point can represent the trend of reflectivity variation in a simple plot, as shown in Figure 2E. The suddenly decreased reflectivity (represented by the color change from green to blue in Figure 2D and by the curved dip in Figure 2E) coincided with the start of vessel dilation. The changes in cortical reflectivity ended approximately at the seizure's end. In spite of the low transparency of the brain tissue, we were able to record the tissue-scattering signal from 2 mm below the surface, which is deeper than the cortical thickness. With fair confidence, we conclude that both ΔR(x,t) and ΔR(t) are more sensitive in signaling the start and the end of the seizure than EEG signals.

Discussion

The 4-AP model of epileptic seizures (Bahar *et. al.*, 2006; Tsytsarev *et. al.*, 2011; Zhao *et. al.*, 2011; Raol and Brooks-Kayal, 2012) allows us to investigate periods of induction, maintenance, and propagation of seizure discharges, and has been extensively studied using different optical methods. It is generally known that epileptic seizures are accompanied by a local increase in cerebral blood flow to the epileptic focus (Zhao *et. al.*, 2011, Hirase *et. al.*, 2004; Santisakultarm *et. al.*, 2011; Schwartz *et. al.*, 2004), but the relationship between seizures and neuronal activity remains unclear. The trigger mechanism of the seizure as a synchronized activity of the neural network is also not very well established. Although it is unlikely that vasodilatation itself can initiate the seizure, fast vasodilatation might be a first indicator of the local biochemical process that accompanies the seizure's beginning. It was proposed by de Vasconcelos *et. al.*, (1995) that nitric oxide triggers vasodilation in response to focal epileptic seizures, but in their work, vasodilatation was observed in a relatively large area, including both the cortex around epileptic foci and also (bilaterally) the substantia nigra and the parafascicular thalamic nucleus. It seems possible that astrocytes' release of glutamate in the area of the epileptic foci plays a causal role in synchronous firing of a large neural population (Carmignoto and Haydon, 2012; Inyushin et al, 2012). Synchronous activity of the astrocytic syncytium can cause changes in the optical features of the cortical tissue that can be observed by OCT.

OCT has been used for *in vivo* brain imaging in animal experiments (Satomura Y. *et. al.*, 2004; Aguirre A. D. *et. al.*, 2006; Rajagopalan U. M. *et. al.*, 2007; Chen Y. *et. al.*, 2009; Sato M. *et. al.*, 2010; Liang *et. al.*, 2011; Lenkov *et. al.*, 2012; M. Eberle *et. al.*, 2012) and provides high spatial resolution and a wide field of view. The modulation of the optical refractive index by the epileptic neuronal activity during a seizure coincides with the observation of surface reflectivity changes. As demonstrated in our experiments, OCT represents a very effective direct optical epilepsy mapping method, with a depth range of about 2 mm. Due to the well-known neurovasculature coupling mechanism, dynamic blood flow changes such as the vasodilatation observed in our experiments may be established as

another effective optical epilepsy mapping method for documenting epilepsy seizure. Theoretically, most blood flow imaging methods, including Doppler OCT and its variants, could be used to record the dynamic blood flow change caused by an epileptic seizure. The recently invented PAM technology has major advantages due to both its high contrast (as high as 40 dB) and its multi-scale imaging capability, which provides a much deeper imaging depth not achievable by other optical imaging technologies. In this demonstration, we used a very simple epilepsy mapping protocol, which does not utilize the full speed of our imaging systems (20,000 A-lines-per-second). It is very straightforward to upgrade the dual contrast imaging system to a 100,000 or 200,000 A-lines-per-second imaging speed, enabling more sophisticated mapping protocols. The dual contrast optical epilepsy mapping method demonstrated in this short communication presents a new tool for epilepsy drug development with small animal models (Raol *et. al.*, 2012). With appropriate modifications, it could be used as an intra-operative tool for determining the boundary of epileptic tissue in epilepsy surgery (Haglund *et. al.*, 2004).

Conclusions

We demonstrate for the first time *in vivo* epilepsy mapping with high spatial and temporal resolution and dual optical contrasts in an animal model. Through the variations in a depth-resolved optical coherence tomography signal with optical scattering contrast, we observed variations of the depth resolved optical reflection signal from epilepsy tissue. Simultaneously, through neurovascular coupling mechanisms and optical absorption contrast, we used photoacoustic signals to document the hemodynamic changes of the microvasculature surrounding the epileptic neurons. The epilepsy mapping results were confirmed by a simultaneously recorded electroencephalogram signal during epileptic seizure. Our new epilepsy mapping tool, with high temporal and spatial resolution and dual optical contrasts, may find many applications, such as in drug development and epilepsy surgery.

Acknowledgments

This work was sponsored in part by National Institutes of Health grants R01 EB008085, R01 CA134539, U54 CA136398, R01 CA157277, R01 CA159959, DP1 EB016986 (NIH Director’s Pioneer Award).. L.W. has a financial interest in Microphotoacoustics, Inc. and Endra, Inc., which, however, did not support this work. K.M. has a financial interest in Microphotoacoustics, Inc., which, however, did not support this work.

References

1. Aguirre AD, Chen Y, Fujimoto JG, Ruvinskaya L, Devor A, Boas DA. Depth-resolved imaging of functional activation in the rat cerebral cortex using optical coherence tomography. Opt Lett. 2006; 31(23):3459–3461. [PubMed: 17099749]
2. Bahar S, Suh M, Zhao M, Schwartz TH. Intrinsic optical signal imaging of neocortical seizures: the ‘epileptic dip’. Neuroreport. 2006; 17(5):499–503. [PubMed: 16543814]
3. Carmignoto G, Haydon PG. Astrocyte calcium signaling and epilepsy. Glia. 2012; 60:1227–1233. [PubMed: 22389222]
4. Chen Y, Aguirre AD, Ruvinskaya L, Devor A, Boas DA, Fujimoto JG. Optical coherence tomography (OCT) reveals depth-resolved dynamics during functional brain activation. J Neurosci Methods. 2009; 30;178(1):162–73.

5. Cohen LB, Lesher S. Optical monitoring of membrane potential: methods of multisite optical measurement. Opt Methods Cell Physiol. 1986; 40:71–99.
6. Craven I, Kotsarini C, Hoggard N. Recent advances in imaging epilepsy. Postgrad Med J. 2010; 86(1019):552–9. [PubMed: 20716588]
7. Eberle M, Reynolds C, Szu J, Wang Hansen A, Hsu M, Islam M, Binder D, Park B. *In vivo* detection of cortical optical changes associated with seizure activity with optical coherence tomography. Biomed Opt Express. 2012; 3:2700–2706. [PubMed: 23162709]
8. Hillman EM, Devor A, Bouchard MB, Dunn AK, Krauss GW, Skoch J, Bacskai BJ, Dale AM, Boas DA. Depth-resolved optical imaging and microscopy of vascular compartment dynamics during somatosensory stimulation. NeuroImage. 2007; 35(1):89–104. [PubMed: 17222567]
9. Hirase H, Creso J, Buzsaki G. Capillary level imaging of local cerebral blood flow in bicuculline-induced epileptic foci. Neuroscience. 2004; 128(1):209–16. [PubMed: 15450368]
10. Haglund MM, Hochman DW. Optical imaging of epileptiform activity in human neocortex. Epilepsia. 2004; 45 (Suppl 4):43–47. [PubMed: 15281958]
11. Hu S, Maslov K, Tsytsarev V, Wang LV. Functional transcranial brain imaging by optical-resolution photoacoustic microscopy. J Biomed Opt. 2009; 14(4):040503. [PubMed: 19725708]
12. Huang D, Swanson EA, Lin CP, Schuman JS, Stinson WJ, Chang W, Hee MR, Flotte T, Gregory K, Puliafito CA, Fujimoto JG. Optical coherence tomography. Science. 1991; 254:1178–118. [PubMed: 1957169]
13. Jonathan E, Enfield J, Leahy MJ. Correlation mapping method for generating microcirculation morphology from optical coherence tomography (OCT) intensity images. J Biophotonics. 2011; 4(9):583–7. [PubMed: 21887769]
14. Inyushin MY, Vol'nova AB, Lenkov DN. Use of a Simplified Method of Optical Recording to Identify Foci of Maximal Neuron Activity in the Somatosensory Cortex of White Rats. Neuroscience and Behavioral Physiology. 2001; 31(2):201–205. [PubMed: 11388374]
15. Inyushin M, Kucheryavykh LY, Kucheryavykh YV, Nichols CG, Buono RJ, Ferraro TN, Skatchkov SN, Eaton MJ. Potassium channel activity and glutamate uptake are impaired in astrocytes of seizure-susceptible DBA/2 mice. Epilepsia. 2010; 51(9):1707–13. [PubMed: 20831751]
16. Inyushin MY, Huertas A, Kucheryavykh YV, Kucheryavykh LY, Tsydzik V, Sanabria P, Eaton MJ, Skatchkov SN, Rojas LV, Wessinger WD. L-DOPA Uptake in Astrocytic Endfeet Enwrapping Blood Vessels in Rat Brain. Parkinsons Dis. 2012; 2012:321406. [PubMed: 22888467]
17. Lee M, Kim D, Shin HS, Sung HG, Choi JH. High-density EEG recordings of the freely moving mice using polyimide-based microelectrode. J Vis Exp. 2011; 11(47):2562. [PubMed: 21248705]
18. Lenkov DN, Volnova AB, Pope ARD, Tsytsarev V. Advantages and limitations of brain imaging methods in the research of absence epilepsy in humans and animal models. J Neurosci Methods. 2013; 212(2):195–202. [PubMed: 23137652]
19. Liang CP, Wierwille J, Moreira T, Schwartzbauer G, Jafri MS, Tang CM, Chen Y. A forward-imaging needle-type OCT probe for image guided stereotactic procedures. Opt Express. 2011; 19(27):26283–94. [PubMed: 22274213]
20. Liao LD, Lin CT, Shih YY, Duong TQ, Lai HY, Wang PH, Wu R, Tsang S, Chang JY, Li ML, Chen YY. Transcranial imaging of functional cerebral hemodynamic changes in single blood vessels using *in vivo* photoacoustic microscopy. J Cereb Blood Flow Metab. 2012; 32(6):938–51. [PubMed: 22472612]
21. Liao LD, Lin CT, Shih YY, Lai HY, Zhao WT, Duong TQ, Chang JY, Chen YY, Li MM. Investigation of the cerebral hemodynamic response function in single blood vessels by functional photoacoustic microscopy. Journal of Biomedical Optics. 2012; 17(6):061210. [PubMed: 22734740]
22. Liao LD, Li ML, Lai HY, Shih Y, Lo YC, Tsang S, Chao PCP, Lin CT, Jaw FS, Chen YY. Imaging brain hemodynamic changes during rat forepaw electrical stimulation using functional photoacoustic microscopy. NeuroImage. 2010; 52(2):562–70. [PubMed: 20362680]

23. Ma HT, Zhao MR, Suh M, Schwartz TH. Hemodynamic Surrogates for Excitatory Membrane Potential Change During Interictal Epileptiform Events in Rat Neocortex. J Neurophysiol. 2009; 101(5):2550–2562. [PubMed: 19244357]
24. Maheswari RU, Takaoka H, Kadono H, Homma R, Tanifuji M. Novel functional imaging technique from brain surface with optical coherence tomography enabling visualization of depth resolved functional structure *in vivo*. Journal of Neuroscience Methods. 2003; 124:83–92. [PubMed: 12648767]
25. Maslov KI, Zhang HF, Hu S, Wang LV. Optical-resolution photoacoustic microscopy for *in vivo* imaging of single capillaries. Optics letters. 2008; 33(9):929–931. [PubMed: 18451942]
26. Mitsueda-Ono T, Ikeda A, InouchiTakaya S, Matsumoto R, Hanakawa T, Sawamoto N, Mikuni N, Fukuyama H, Takahashi RJ. Amygdalar enlargement in patients with temporal lobe epilepsy. Neurol Neurosurg Psychiatry. 2011; 82(6):652–7.
27. Pereira de Vasconcelos A, Baldwin RA, Wasterlain CG. Nitric oxide mediates the increase in local cerebral blood flow during focal seizures (quantitative autoradiography/N--nitro-L-arginine/ methylene blue/rat). PNAS. 1995; 92:3175–3179. [PubMed: 7536926]
28. Pinto KG, Scorza FA, Arida RM, Cavalheiro EA, Martins LD, Machado HR, Sakamoto AC, Terra VC. Sudden unexpected death in an adolescent with epilepsy: All roads lead to the heart? Cardiol J. 2011; 18(2):194–6. [PubMed: 21432828]
29. Rajagopalan UM, Tanifuji M. Functional optical coherence tomography reveals localized layer-specific activations in cat primary visual cortex *in vivo*. Opt Lett. 2007; 32(17):2614–2616. [PubMed: 17767323]
30. Rao B, Yu L, Chiang HK, Zacharias LC, Kurtz RM, Kuppermann BD, Chen Z. Imaging pulsatile retinal blood flow in human eye. Journal of Biomedical Optics. 2008; 13(4):040505. [PubMed: 19021308]
31. Rao B, Li L, Maslov K, Wang LV. Hybrid-scanning optical-resolution photoacoustic microscopy for in vivo vasculature imaging. Optics Letters. 2010; 35:1521–1523. [PubMed: 20479795]
32. Rao, Bin; Li, Li; Maslov, Konstantin; Wang, Lihong V. *In vivo*, dual-modality imaging of mouse eyes: optical coherence tomography and photoacoustic microscopy within a single instrument. Proc of SPIE. 2010; 7550:75501Q1–5.
33. Raol YH, Brooks-Kayal AR. Experimental models of seizures and epilepsies. Prog Mol Biol Transl Sci. 2012; 105:57–82. [PubMed: 22137429]
34. Sato M, Nomura D, Tsunenari T, Nishidate I. *In vivo* rat brain measurements of changes in signal intensity depth profiles as a function of temperature using wide-field optical coherence tomography. Applied Optics. 2010; 49(30):20.
35. Santisakultarm TP, Schaffer CB. Optically quantified cerebral blood flow. J Cereb Blood Flow Metab. 2011; 31(6):1337–8. [PubMed: 21364601]
36. Satomura Y, Seki J, Ooi Y, Yanagida T, Seiyama A. *In vivo* imaging of the rat cerebral microvessels with optical coherence tomography. Clin Hemorheol Microcirc. 2004; 31(1):31–40. [PubMed: 15272151]
37. Schwartz TH, Chen LM, Friedman RM, Spencer DD, Roe AW. Intraoperative optical imaging of human face cortical topography: a case study. Neuroreport. 2004; 28;15(9):1527–31.
38. Schwartz TH, Bonhoeffer T. *In vivo* optical mapping of epileptic foci and surround inhibition in ferret cerebral cortex. Nat Med. 2001; 7(9):1063–7. [PubMed: 11533712]
39. Tsytsarev V, Bernardelli C, Maslov KI. Living Brain Optical Imaging: Technology, Methods and Applications. J Neuroscience and Neuroengineering. 2012; 1(2):180–192.
40. Tsytsarev V, Maslov KI, Yao J, Parameswar AR, Demchenko AV, Wang LV. *In vivo* imaging of epileptic activity using 2-NBDG, a fluorescent deoxyglucose analog. J eurosci Methods. 2012; 203(1):136–40.
41. Tsytsarev V, Fukuyama H, Pope D, Pumbo E, Kimura M. Optical imaging of interaural time difference representation in rat auditory cortex. Front Neuroengineering. 2009; 2(2)
42. Tsytsarev V, Pope D, Pumbo E, Yablonskii A, Hofmann M. Study of the cortical representation of whisker directional deflection using voltage-sensitive dye optical imaging. Neuroimage. 2010; 53(1):233–238. [PubMed: 20558304]

43. Tsytsarev V, Premachandra K, Takeshita D, Bahar S. Imaging cortical electrical stimulation *in vivo*: fast intrinsic optical signal versus voltage-sensitive dyes. Opt Lett. 2008; 33(9):1032–1034. [PubMed: 18451977]
44. Tsytsarev V, Hu S, Yao J, Maslov KI, Barbour DL, Wang LV. Photoacoustic microscopy of microvascular responses to cortical electrical stimulation. J Biomedical Optics. 2011; 16(7): 076002.
45. Wang LV. Prospects of photoacoustic tomography. Medical Physics. 2008; 35 (12):5758–5767. [PubMed: 19175133]
46. Wang LV. Multiscale photoacoustic microscopy and computed tomography. Nature Photon. 2009; 3:503–509.
47. Wang LV, Song Hu. Photoacoustic tomography: *in vivo* imaging from organelles to organs. Science. 2012; 335:1458–1462. [PubMed: 22442475]
48. Wang XD, Pang YJ, Ku G, Xie XY, Stoica G, Wang LV. Noninvasive laser-induced photoacoustic tomography for structural and functional *in vivo* imaging of the brain Nat. Biotechnol. 2003; 21(7): 803–806.
49. Yao J, Xia J, Maslov KI, Nasiriavanaki M, Tsytsarev V, Demchenko AV, Wang LV. Noninvasive photoacoustic computed tomography of mouse brain metabolism *in vivo*. Neuroimage. 2012; 1(64):257–66. [PubMed: 22940116]
50. Zhao M, Nguyen J, Ma H, Nishimura N, Schaffer CB, Schwartz TH. Preictal and Ictal Neurovascular and Metabolic Coupling Surrounding a Seizure Focus. The Journal of Neuroscience. 2011; 31(37):13292–13300. [PubMed: 21917812]

ETHICAL STANDARDS

- The authors declare that all experiments on human subjects were conducted in accordance with the Declaration of Helsinki http://www.wma.net and that all procedures were carried out with the adequate understanding and written consent of the subjects.
- The authors also certify that formal approval to conduct the experiments described has been obtained from the human subjects review board of their institution and could be provided upon request.
- If the studies deal with animal experiments, the authors certify that they were carried out in accordance with the National Institute of Health Guide for the Care and Use of Laboratory Animals (NIH Publications No. 80-23) revised 1996 or the UK Animals (Scientific Procedures) Act 1986 and associated guidelines, or the European Communities Council Directive of 24 November 1986 (86/609/EEC).
- The authors also certify that formal approval to conduct the experiments described has been obtained from the animal subjects review board of their institution and could be provided upon request.
- The authors further attest that all efforts were made to minimize the number of animals used and their suffering.
- If the ethical standard governing the reported research is different from those guidelines indicated above, the authors must provide information in the submission cover letter about which guidelines and oversight procedures were followed.
- The Editors reserve the right to return manuscripts in which there is any question as to the appropriate and ethical use of human or animal subjects.

Highlights

- Epileptic seizures in the mice neocortex were induced in vivo by intracortical injection of 4-aminopyridine
- Optical coherence tomography and photoacoustic images of the cortex were acquired simultaneously
- We have observed a decrease in optical scattering caused by the epileptic seizures
- We have observed vasodilatation of the small blood caused by the epileptic seizures

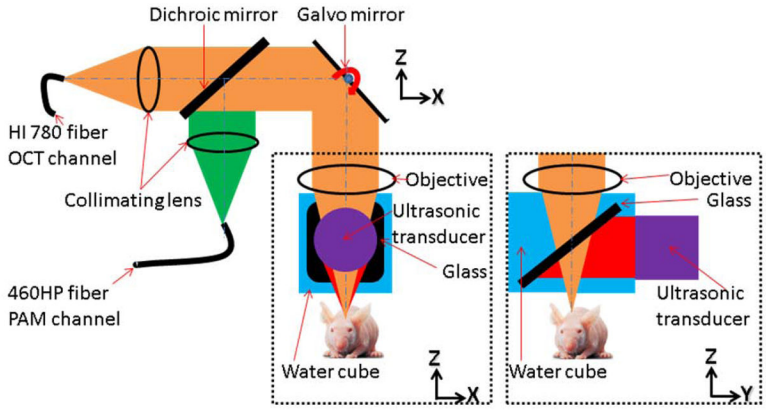

Figure 1.

Schematic of the dual-modality OCT/PAM imaging probe: The OCT system was connected to the dual-modality probe through a single-mode fiber (HI-780, Thorlabs). The 532 nm pulsed laser was connected to the probe with another single-mode fiber (460-HP, Thorlabs). The collimated OCT sample and the 532 nm PAM excitation beams were combined using a dichroic mirror and focused by a microscope objective (NA 0.1) at 200 μm below the tissue surface. Fast optical scanning along one axis (B-scan) was done by a galvanometer mirror. Upon the absorption of the laser pulse by the tissue, photoacoustic waves were generated. Thereafter, the waves were reflected by a glass plate placed at 45 degrees between the objective and the animal, and detected by the cylindrically focused ultrasonic transducer (GE, 25 MHz bandwidth). The whole probe was attached to a one-dimensional mechanical stage, which scanned perpendicularly to the fast optical scan axis. The OCT A-line image and the PAM A-line image were acquired sequentially for each A-line.

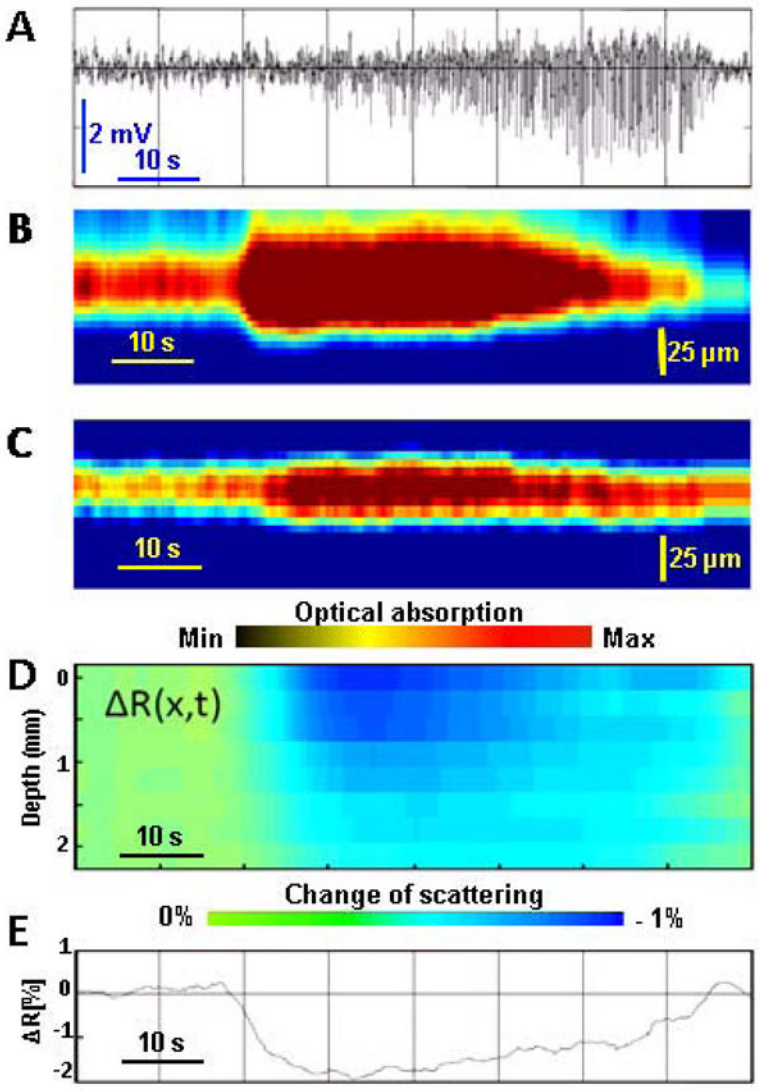

Figure 2.

Time course of an epileptic seizure development: A. Electroencephalogram (EEG) of the epileptic seizure. B. Plot of maximum amplitude projection (MAP) images from PAM versus time for a vein, capturing the vasodilatation process, which was well correlated with EEG signals. C. Plot of MAP images of PAM versus time of an artery, capturing a similar vasodilatation process during seizure, but with a reduced amplitude and prolonged time. D. Depth-resolved reflectivity change ΔR(x,t), where x represents depth and t represents time. E. Averaged optical reflectivity change ΔR(t) of the affected brain cortex tissue, showing how it is affected by the seizure.